~205

Copy
RM L52K14b

CONFIDENTIAL

53-35-61

NACA

RESEARCH MEMORANDUM

FLIGHT INVESTIGATION OF A SUPERSONIC CANARD

MISSILE EQUIPPED WITH AN AUXILIARY DAMPING-IN-PITCH

CONTROL SYSTEM

By Martin T. Moul

Langley Aeronautical Laboratory
Langley Field, Va.

Nasa Tech Pub Announcement #109

29 NOV 56

GRADE OF OFFICER MAKING CHANGE)

This material contains information affecting the National Defense of the United States within the meaning
of the espionage laws, Title 18, U.S.C., Secs. 793 and 794, the transmission or revelation of which in any
manner to an unauthorized person is prohibited by law.

NATIONAL ADVISORY COMMITTEE
FOR AERONAUTICS

WASHINGTON

February 2, 1953

CONFIDENTIAL

CONFIDENTIAL

NATIONAL ADVISORY COMMITTEE FOR AERONAUTICS

RESEARCH MEMORANDUM

FLIGHT INVESTIGATION OF A SUPERSONIC CANARD

MISSILE EQUIPPED WITH AN AUXILIARY DAMPING-IN-PITCH

CONTROL SYSTEM

By Martin T. Moul

SUMMARY

A 60° delta-wing canard missile equipped with a rate-damping system to dampen longitudinal oscillations has been flight-tested through a Mach number range of 0.70 to 1.85 with a static margin at supersonic speeds of approximately 50 percent of the mean aerodynamic chord. Experimental transient responses to step deflections of the canard surfaces are presented to illustrate the auxiliary damping in pitch provided by the rate system. A comparison is made of experimental transient responses and theoretical transient responses computed from the linearized equations of motion by application of operational-calculus methods and servomechanism theory. Some missile aerodynamic characteristics are presented as functions of Mach number.

The rate-gyro—servo system, acting through wing-tip controls to provide auxiliary damping in pitch, was effective in damping the transient responses and caused the oscillations to be almost completely damped at the end of $1\frac{1}{2}$ cycles. The comparison between measured and computed responses showed that the theoretical method provides an accurate means of predicting missile response if experimental stability derivatives and rate-system characteristics are used. The experimental data indicated that the addition of tip controls to the canard missile caused a varying lift-curve slope during the oscillatory response, reduced the pitching effectiveness at transonic speeds, but had no appreciable effect on trim drag.

INTRODUCTION

Investigations of the performance characteristics of an automatically controlled canard missile configuration being conducted by the Langley Pilotless Aircraft Research Division have indicated that the aerodynamic

CONFIDENTIAL

damping in pitch of the configuration determined from rocket-powered model tests (refs. 1 and 2) is inadequate for certain guidance problems. A theoretical study (ref. 3) has shown that the missile dynamic performance characteristics are improved by the addition of auxiliary damping introduced by a rate-gyro—servo control system through either canard fins or wing-tip controls. The present investigation, with the rate-damping system acting through wing-tip controls, was undertaken to verify experimentally the results indicated in reference 3.

Auxiliary-damping data are presented as transient responses to a step-function control-surface input for a Mach number range of 0.70 to 1.85. Some longitudinal aerodynamic characteristics are also presented for the Mach number range of the flight.

SYMBOLS

c	wing chord, ft
$\bar{c}$	wing mean aerodynamic chord, ft
S	total wing area in one plane including body intercept, sq ft
t	time, sec
h	altitude, ft
m	mass, slugs
W	weight, lb
I_y	moment of inertia about Y-axis, slugs-ft^2
g	acceleration due to gravity, ft/sec^2
V	velocity of model, ft/sec
V_c	speed of sound in air, ft/sec
M	Mach number, V/V_c
q	dynamic pressure, lb/sq ft
θ	angle of pitch, deg
α	angle of attack, deg

δ control-surface deflection, deg

$\dot{\theta}$ pitching velocity, deg/sec

a_n/g normal accelerometer reading

a_l/g longitudinal-accelerometer reading, deceleration positive

C_L lift coefficient, $\left(\dfrac{a_n}{g}\cos\alpha - \dfrac{a_l}{g}\sin\alpha\right)\dfrac{W}{qS}$

C_D drag coefficient, $\left(\dfrac{a_l}{g}\cos\alpha + \dfrac{a_n}{g}\sin\alpha\right)\dfrac{W}{qS}$

C_m pitching-moment coefficient,

$$\frac{\text{Pitching moment about center of gravity}}{qS\bar{c}}$$

$K = \dfrac{C_{m_{\delta_t}}}{C_{m_{\delta_s}}}$

p Laplace transform variable corresponding to the differential operator $D \equiv \dfrac{d}{dt}$

ω frequency of oscillations, radians/sec

Subscripts:

trim   trim or steady-state condition

s   canard control surface

t   wing-tip control surface

e   equivalent

$\dot{\alpha}$ $\dfrac{d\alpha}{dt}\dfrac{\bar{c}}{2V}$

q $\dfrac{\dot{\theta}\bar{c}}{2V}$

$\alpha, \delta, \dot{\alpha}, q$ partial derivatives

APPARATUS AND METHODS

Model Description

The missile fuselage consisted of a 7-inch-diameter cylindrical section and ogival nose and tail cones. Triangular wings were mounted on the body in a cruciform arrangement. Smaller triangular fins were mounted near the nose in line with the horizontal wing as all-movable control surfaces. The model arrangement and principal dimensions are presented in figure 1.

The triangular wings were swept back $59^\circ 32'$ and had a modified double-wedge airfoil section. The small triangular canard fins were swept back 60° and had the same airfoil section as the wings. Half-delta fins with the leading edge swept back $59^\circ 32'$ and of a double-wedge section were mounted at the tips of the horizontal wings as all-movable controls. The wings were constructed of solid magnesium and the two sets of control surfaces of steel. Details of the wing and control surfaces are presented in figure 2. It may be noted in figure 2 that the tip controls are slightly smaller than the replaced wing tip. A photograph of the model is presented as figure 3 and physical characteristics are presented in table I.

Control Systems

The auxiliary-damping system consisted of a rate gyroscope, proportional low-lag pneumatic servomotor, slide valve, air accumulator, regulator, purifier, and linkages. All the components, with the exception of the accumulator, regulator, and purifier, were located immediately rearward of the wings and occupied an 8-inch section of the fuselage. A photograph of the system installation is presented as figure 4(a).

Rate-gyro signals were transmitted by mechanical linkages as shown by the schematic diagram in figure 4(b), through the air valve, servomotor, and torque rod to produce deflections of the wing-tip control surfaces proportional to pitching velocity. The motion of the gyro gimbal was spring-restrained and damped by two dash pots. A Lanchester damper was used to damp the servo motion. The mechanical linkage between the servomotor and torque rod was designed to limit the tip controls to maximum deflections of $\pm 10^\circ$. A block diagram of the missile and auxiliary-damping system is presented in figure 4(c).

The canard fins were deflected in a continuous square wave with deflections of 5.2° and -4.8° and a dwell time of 0.75 second, to provide pitch disturbances. A hydraulic pulsing system supplied from an accumulator actuated the controls.

Instrumentation

The model was equipped with an NACA nine-channel telemeter which transmitted continuous records of normal (two ranges), longitudinal, and transverse accelerations, angle of attack, canard control deflection, wing-tip control deflection, total pressure, and a calibrated static pressure. A free-floating vane extending from the nose on a sting measured angle of attack, and a tube extending below the body measured total pressure. The positions of these two instruments are shown in figure 1. The measured angles of attack were corrected to the missile center of gravity by the method of reference 4.

The model trajectory was determined by a modified SCR 584 type radar tracking unit. A radiosonde released at the time of flight measured temperatures and atmospheric pressures through the altitude range traversed by the model. Model velocity was obtained from a CW Doppler velocimeter and from total and radiosonde static pressures.

Launching

The model was boosted to supersonic speeds by two solid propellant rocket motors of 20,000-pounds-seconds total impulse and 3-second burning time which were ignited simultaneously. The method of launching was similar to that described in reference 1, with the launching angle being changed to 60°.

Method of Analysis

In reference 3 several methods were presented for studying missile automatic-control-system performance by using frequency-response and transient-response characteristics. The method for calculating transient responses from the linearized equations of motion is used herein to provide a comparison of experimental and theoretical results. The method, as adapted for solving by the Reeves Electronic Analog Computer (REAC) is presented here.

The block diagram representing the system is similar to that of reference 3, except that the attitude-autopilot loop is excluded and an airframe transfer function α/θ is added:
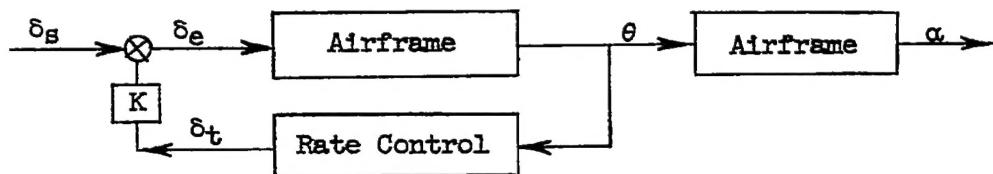
Airframe transfer functions were calculated by using the method of operational calculus from the longitudinal equations of motion for two degrees of freedom as used in reference 3. The simplified $\left(C_{L_{\delta_s}} = 0\right)$ open-loop transfer functions are

$$\frac{\theta}{\delta_e} = \frac{\left(\frac{mV}{57.3qS}\, C_{m_{\delta_s}}\right)p + C_{L_\alpha}C_{m_{\delta_s}}}{\left\{p\left[\left(\frac{mV}{57.3qS}\right)\left(\frac{I_y}{57.3qS\bar{c}}\right)p^2 - \left(\frac{mV}{57.3qS}\, C_{m_q}\, \frac{\bar{c}}{2V} + \frac{mV}{57.3qS}\, C_{m_{\dot\alpha}}\, \frac{\bar{c}}{2V} - C_{L_\alpha}\frac{I_y}{57.3qS\bar{c}}\right)p - \left(\frac{mV}{57.3qS}\, C_{m_\alpha} + C_{L_\alpha}C_{m_q}\, \frac{\bar{c}}{2V}\right)\right]\right\}} \tag{1}$$

$$\frac{\alpha}{\theta} = \frac{p}{p + C_{L_\alpha}\, \frac{mV}{57.3qS}} \tag{2}$$

Experimental stability derivatives of the configuration, reported in reference 2, and flight conditions and model characteristics from this investigation were used in determining the transfer functions. Values of the aerodynamic quantities used in the calculations are listed in table II. The aerodynamic derivatives for a Mach number of 1.81 were obtained by extrapolating the data of reference 2. Tip-control data were obtained from the results of two tests reported in references 5 and 6.

The rate-gyro—servo system was originally a single-degree-of-freedom system with the natural frequency changed from 88 to 221 radians per second. Because the force provided by the servomotor was only 30 pounds, the maximum allowable aerodynamic hinge moment was small. As a result an inertia damper was added to the servomotor to reduce the magnitudes of the initial overshoot of the servo response. This modification enabled a higher static sensitivity $\delta_t/\dot\theta$ to be used. From a consideration of hinge moments and pitching velocities, a static sensitivity $\delta_t/\dot\theta$ of 0.2 was chosen as the maximum feasible value. This value is in line with the results of reference 3 that high static sensitivities yield more satisfactory responses than small sensitivities for this range of gyro-servo dynamics.

With this sensitivity the rate-gyro—servo system was then tested and a transient response to a step deflection of the gyro gimbal

was obtained. The modes of motion were recognized in the response, and an equation was fitted to the curve by a trial-and-error method. The system transfer function, determined from this equation by the methods of operational calculus, is

$$\frac{\delta_t}{\theta} = \frac{-0.14p\left(p^2 - 6{,}386p - 2{,}778{,}600\right)}{\left(p^3 + 70p^2 + 49{,}825p + 1{,}945{,}000\right)} \qquad (3)$$

The tip-control deflection δ_t was fed back into the system as an equivalent canard deflection $K\delta_t$ where $K = \dfrac{C_{m_{\delta_t}}}{C_{m_{\delta_s}}}$. The operations in solving the equations to determine transient responses to a δ_s input of 5° were performed by the REAC and the results were obtained from recording elements.

Accuracy

Inaccuracies in the experimental data result from errors in telemeter equipment and radar. The measured quantities are believed to be accurate within the following limits:

M	Limit of Accuracy					
	M	α, deg	δ_s, deg	δ_t, deg	C_L	C_D
0.8	±0.03	±0.2	±0.2	±0.6	±0.029	±0.014
1.8	±.02	±.2	±.2	±.6	±.004	±.002

The REAC solutions of α and δ_t are believed to be accurate within ±0.1° and ±0.2°, respectively.

RESULTS AND DISCUSSION

Damping Characteristics

Effect of auxiliary damping in pitch on model response.- In order to show how this rate-gyro—servo control system damped the model oscillations, some experimental angle-of-attack transient responses to a 5° step input of the canard surfaces are presented in figure 5 for Mach

numbers 1.81, 1.32, 0.97, 0.71, and 0.72. Results of REAC calculations
are also presented to show the model angle-of-attack transient responses
which could be expected if no auxiliary damping were provided. The
increase in damping is apparent with the experimental responses being
almost completely damped at the end of $1\frac{1}{2}$ cycles at all Mach numbers. In

addition to providing a more satisfactory response to autopilot command
signals, the missile with auxiliary damping experienced a reduction in
maximum normal loads of about 33 percent, an important consideration for
maneuvering flight at high Mach number. An effect of altitude was obtained
when the model accelerated to a Mach number of 0.72 during descent. At
the lower altitude the oscillations were damped in a shorter time as the
result of a higher model natural frequency.

Comparison of experimental and theoretical transient responses.-
In figure 6 measured angle-of-attack and tip-control transient responses
to a 5° step input of the canard surfaces are compared with REAC solutions
of closed-loop transient responses at Mach numbers of 1.81 and 0.71. At
a Mach number of 1.81 the experimental transient response has a higher
steady-state angle of attack and lower natural frequency than the com-
puted response; thus a possible difference in C_{m_α} is indicated. Exper-
imental data were not available above a Mach number of 1.45 in refer-
ence 2, so that errors may have been incurred by extrapolations of the
derivatives for the calculations to a Mach number of 1.81. The damping
of the responses is in good agreement indicating the validity of the
theoretical method for predicting damping characteristics of a missile
equipped with a rate-damping control system.

The tip-control deflections at M = 1.81 are in good agreement
except for the maximum values. The tip controls of the model were limited
to deflections of ±10° because of hinge-moment considerations.

At a Mach number of 0.71 the experimental and computed responses are
in good agreement, except for a small difference in natural frequencies.

Rate-gyro—servo response characteristics.- The gyro-servo transient
response presented in figure 7 was obtained by measuring the tip-control
deflection when a step input was applied to the gyro gimbal. The curve
was fitted by an analytical expression from which the transfer function
was obtained. A comparison with the gyro-servo response given in figure 11
of reference 3 indicates the effects of modifications to the rate system.
A damping mode and increased natural frequency may be noted.

Because of servo-energy hinge-moment considerations discussed pre-
viously, the dynamics of the gyro-servo system of this test were altered
so as to decrease the maximum control deflections. This difference in
control deflections may be noted in figure 8, in which model angle-of-attack

and tip-control-deflection transient responses to a 5° step input of the canard controls are presented for a Mach number of 1.81. The angle-of-attack responses indicate that the auxiliary-damping system of this test did not damp the oscillations as well as the original gyro-servo system might have with the use of higher initial tip-control deflections.

Aerodynamic Characteristics

All the experimental data of this investigation occurred at a reduced frequency $\frac{\omega \overline{c}}{2V} \leq 0.013$ and should be free of unsteady-lift effects.

Lift-curve slope.- Model lift-curve slope C_{L_α} was determined from the lift-coefficient and angle-of-attack time histories by the method of least squares and is presented in figure 9. A large difference is noted between the data for increasing and decreasing α. This difference may be due to a nonlinear lift curve or possibly to a tip-control effect. The existence of a nonlinear lift curve was noted in reference 1 and the data for the lower angle-of-attack range are presented. This difference in C_{L_α} may have resulted from a tip-control effect since a majority of the control responses occur during the times of increasing α. Computations were made to determine the magnitude of lift due to rate of control deflection but the contribution of this term to the model lift was found to be negligible. The C_{L_α} at decreasing α is in fair agreement with that of reference 2.

Steady-state angles of attack, lift coefficient, and tip-control deflection.- The steady-state angles of attack, lift coefficients, and tip-control deflections are presented in figures 10, 11, and 12, respectively, as a function of Mach number for the two canard deflections. The data show a gradual variation of angle of attack and lift coefficient with Mach number with the exception of Mach number 0.92, where a larger trim angle of attack and lift coefficient are noted. Tip-control deflections increased with increasing Mach number from 0.8° at M = 0.72 to 3.5° at M = 1.86. At the lower speeds there is a considerable scatter of the control-deflection data, but the scatter is within the accuracy of the data (±0.6°).

Steady-state angle of attack per unit control deflection.- From the α_{trim} curves, the steady-state angle of attack per unit control deflection was determined and is presented in figure 13. A comparison with $\frac{\Delta\alpha_{trim}}{\Delta\delta_s}$ from reference 2 (for the same center-of-gravity location)

shows that auxiliary damping has little effect upon control effectiveness at supersonic speeds. At transonic speeds there was a large reduction

in $\frac{\Delta\alpha_{trim}}{\Delta\delta_g}$ with the addition of auxiliary damping.

At four Mach numbers calculated values of $\frac{\Delta\alpha_{trim}}{\Delta\delta_g}$ from the experi-

mental data of reference 2 are modified to include the pitching-moment contribution of the tip controls. The test results were larger at supersonic speeds and lower at transonic speeds than the calculated values. The indication is that the two configurations differed somewhat in either C_{m_α} or $C_{m_{\delta_g}}$, as was suggested in the discussion of figure 6.

Trim drag coefficient.- Trim drag coefficient is presented in figure 14 with the trim drag coefficient for the model of reference 2. The data show that the addition of rate damping incurred no drag penalty. The differences in the values at subsonic speeds may be mainly attributed to inaccuracies of Mach number and the longitudinal accelerometer at low speeds.

CONCLUSIONS

The results of a flight investigation of a canard missile having a static margin at supersonic speeds of approximately 50 percent $\bar{c}$ and equipped with a rate-gyro—servo control system to supplement the inherent aerodynamic damping in pitch indicate the following conclusions:

1. Whereas the canard missile was normally lightly damped in the pitching mode, the addition of the rate-damping system to the missile caused the transient responses to be nearly completely damped at the end of $1\frac{1}{2}$ cycles at all Mach numbers.

2. The experimental and calculated responses were in good agreement indicating that the theoretical method provides an accurate means of predicting missile response when a rate-gyro—servo control system is used to provide additional damping in pitch.

3. The experimental data indicated a difference in lift-curve slope during the oscillatory response which may be attributed to either a nonlinear or tip-control effect. Pitching effectiveness as measured by the steady-state angle of attack produced per unit control deflection was

decreased at transonic speeds by the inclusion of the rate-damping control system. The pitching effectiveness at supersonic speeds was not affected. No differences in trim drag were noted due to the addition of the rate-damping control damping.

Langley Aeronautical Laboratory,
    National Advisory Committee for Aeronautics,
        Langley Field, Va.

REFERENCES

1. Zarovsky, Jacob, and Gardiner, Robert A.: Flight Investigation of a Roll-Stabilized Missile Configuration at Varying Angles of Attack at Mach Numbers Between 0.8 and 1.79. NACA RM L50H21, 1951.

2. Niewald, Roy J., and Moul, Martin T.: The Longitudinal Stability, Control Effectiveness, and Control Hinge-Moment Characteristics Obtained From a Flight Investigation of a Canard Missile Configuration at Transonic and Supersonic Speeds. NACA RM L50I27, 1950.

3. Nelson, Walter C., and Passera, Anthony L.: A Theoretical Investigation of the Influence of Auxiliary Damping in Pitch on the Dynamic Characteristics of a Proportionally Controlled Supersonic Canard Missile Configuration. NACA RM L50F30, 1950.

4. Mitchell, Jesse L., and Peck, Robert F.: An NACA Vane-Type Angle-of-Attack Indicator for Use at Subsonic and Supersonic Speeds. NACA RM L9F28a, 1949.

5. Martz, C. William, Church, James D., and Goslee, John W.: Rocket-Model Investigation To Determine the Force and Hinge-Moment Characteristics of a Half-Delta Tip Control on a 59° Sweptback Delta Wing Between Mach Numbers of 0.55 and 1.43. NACA RM L52H06, 1952.

6. Moul, Martin T., and Baber, Hal T., Jr.: The Longitudinal Stability and Control Characteristics of a 60° Delta-Wing Missile Having Half-Delta Tip Controls As Obtained From a Free-Flight Investigation at Transonic and Supersonic Speeds. NACA RM L52H14, 1952.

TABLE I

MISSILE PHYSICAL CHARACTERISTICS

Weight and balance:
  Weight, lb   110
  Center of gravity, station in inches 59.9
  Pitch moment of inertia, slug-ft^2 . . . .   17.8

Wing:
  Area in one plane including body intercept, sq ft 2.82
  Mean aerodynamic chord, ft 1.46
  Thickness ratio at wing-body juncture 0.03

Canard control:
  Exposed area, two fins, sq ft 0.19
  Root chord, ft 0.58
  Thickness ratio at fin-body juncture 0.03

Tip control:
  Exposed area, two fins, sq ft 0.17
  Root chord, ft 0.53
  Thickness ratio 0.03

TABLE II

AERODYNAMIC DERIVATIVES FOR THEORETICAL RESPONSES

[The aerodynamic derivatives, as used in the calculations
and tabulated below, are per degree measure. The static
margin was approximately 50 percent $\bar{c}$ at supersonic
speeds.]

Mach number	C_{L_α}	C_{m_α}	C_{m_q}	$C_{m_{\dot\alpha}}$	$C_{L_{\delta_s}}$	$C_{m_{\delta_s}}$	$C_{m_{\delta_t}}$
0.71	0.0465	-0.0182	-0.306	-0.034	0	0.0097	-0.0055
.97	.0533	-.0240	-.175	-.020	0	.0143	-.0073
1.32	.0472	-.0235	-.189	-.021	0	.0130	-.0037
1.81	.0365	-.0184	-.153	-.017	0	.0105	-.0027

NACA
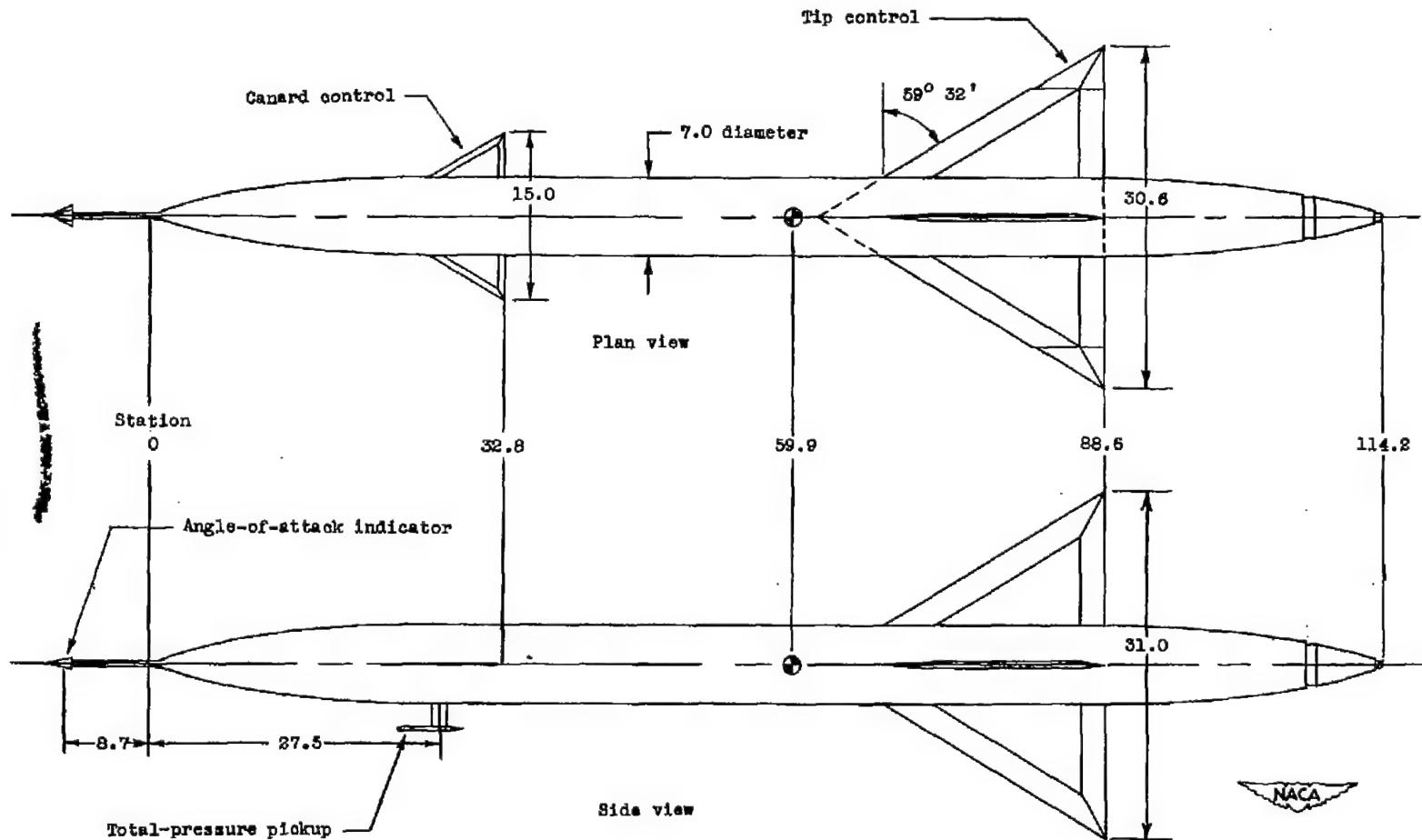
Figure 1.- Model arrangement. All dimensions are in inches.
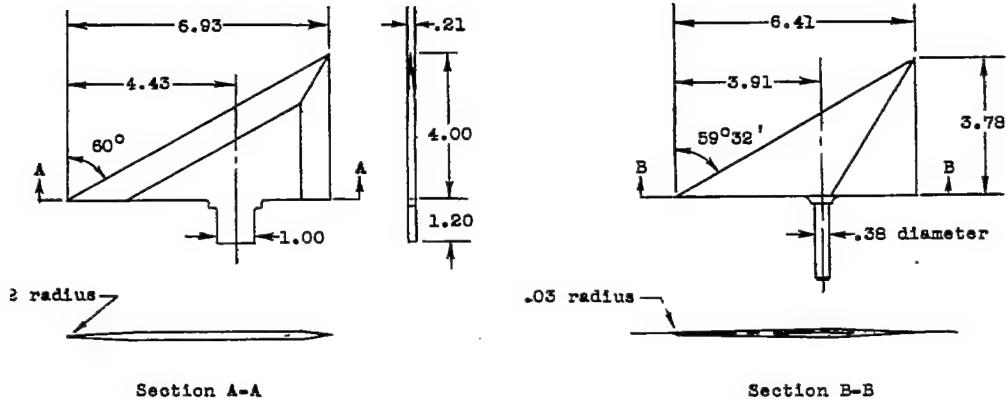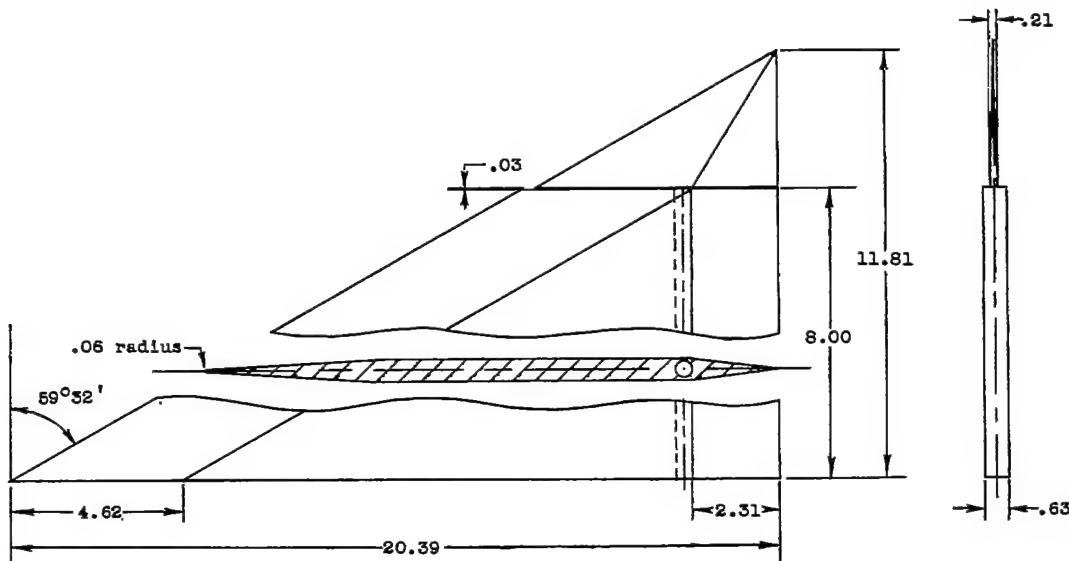
Figure 2.- Detail of wing and control surfaces.   All dimensions are in
inches.
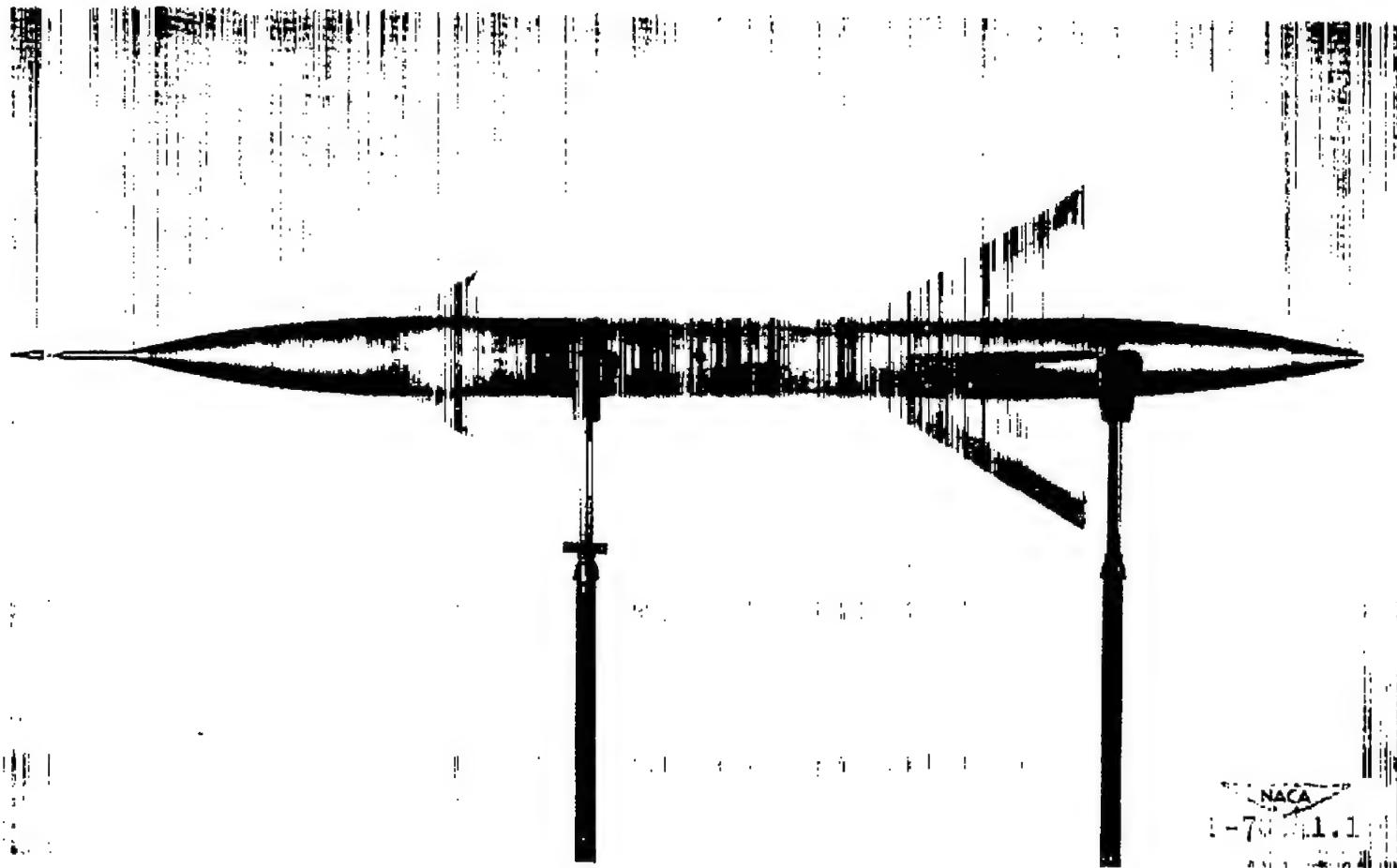
Figure 3.- Missile plan view.

(a) Rate-gyro—servo system installed in missile.

Figure 4.- Rate-gyro—servo system.
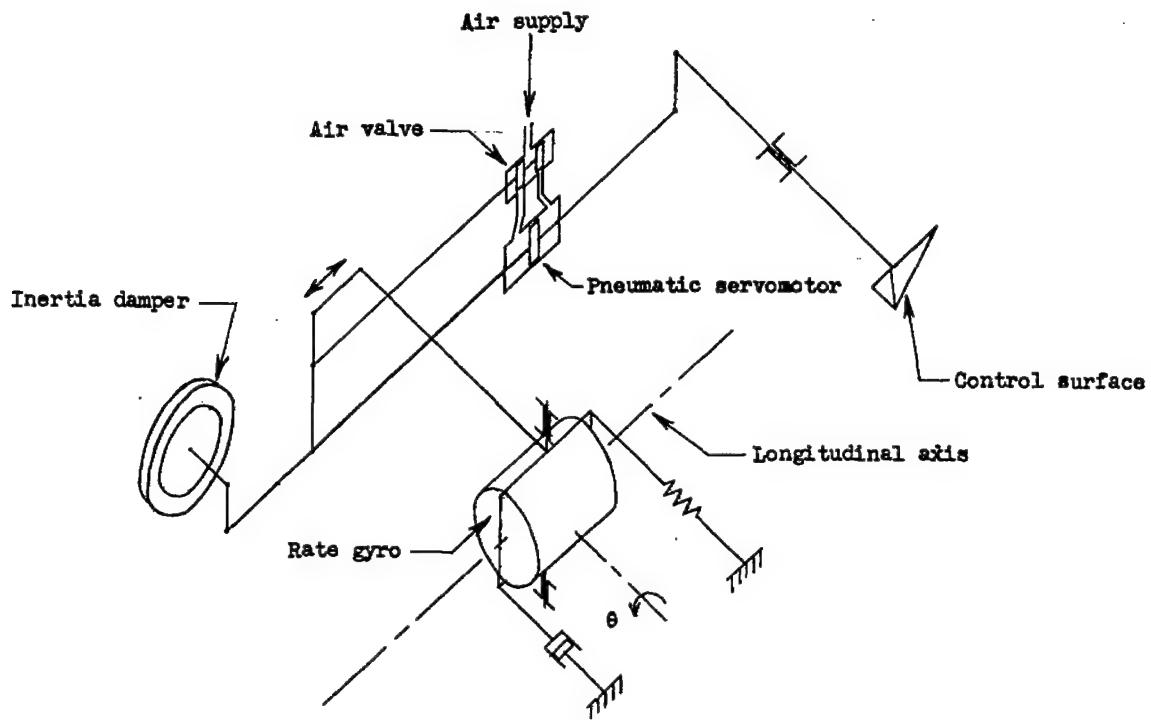
(b) Schematic diagram of components and linkages.
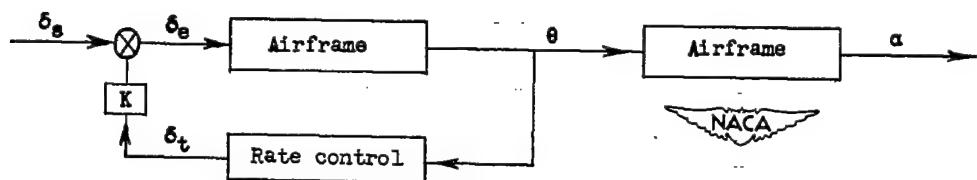
(c) Block diagram of auxiliary-damping system incorporated in missile.

Figure 4.- Concluded.
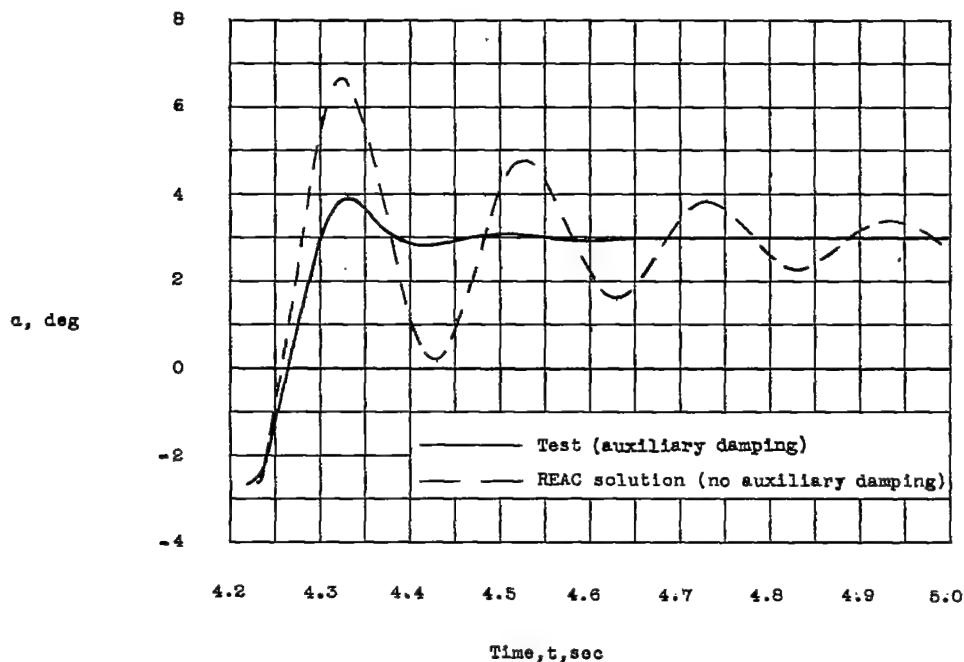
(a) M = 1.81; h = 5,000 feet.
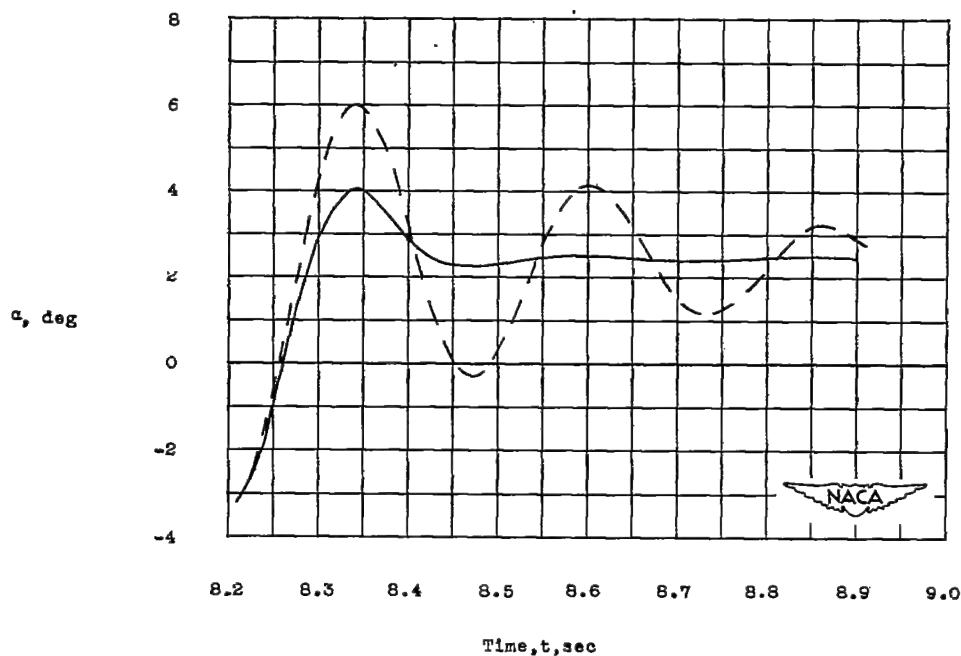
(b) M = 1.32; h = 9,500 feet.

Figure 5.- Effect of auxiliary damping in pitch on model response.
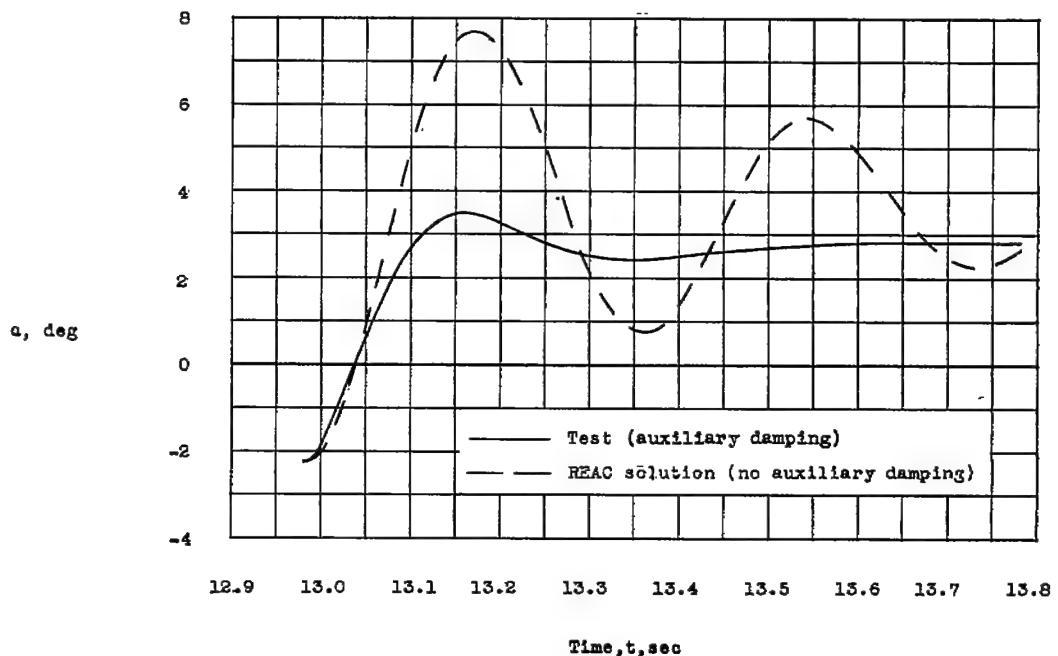
(c) M = 0.97; h = 13,000 feet.
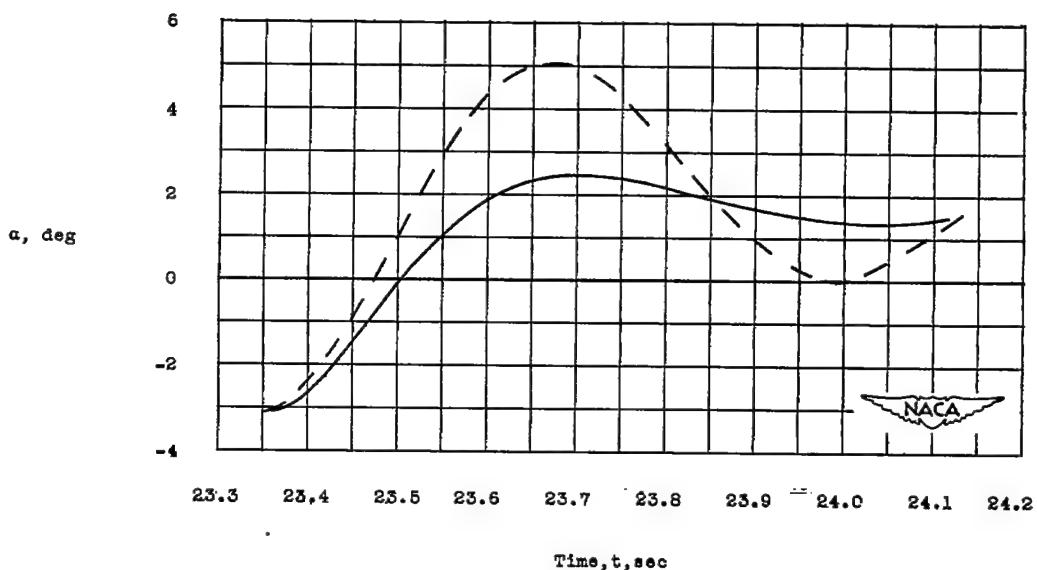
(d) M = 0.71; h = 17,000 feet.

Figure 5.- Continued.

α, deg
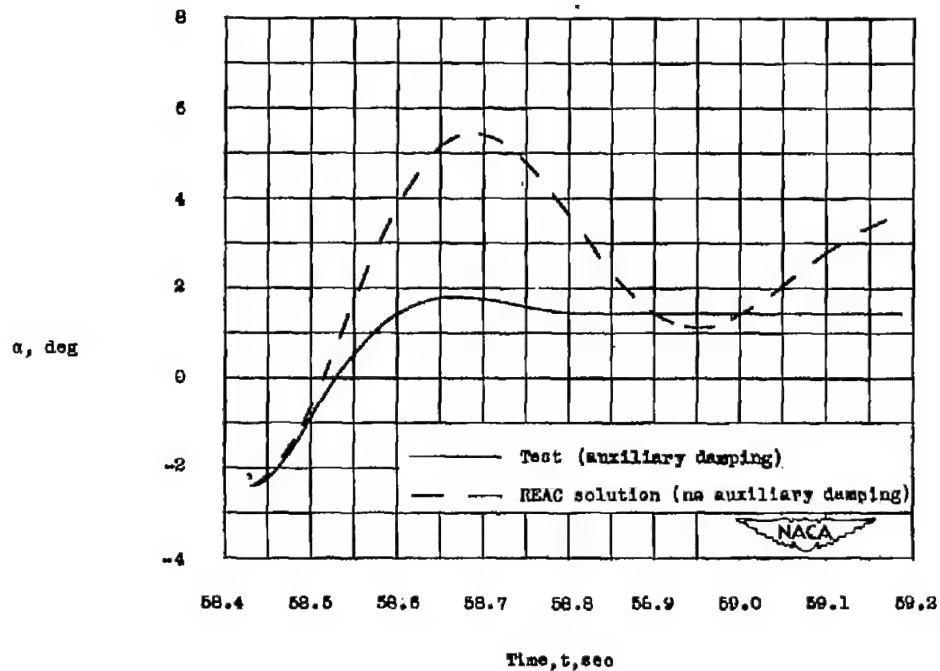
(e) M = 0.72; h = 6,000 feet.

Figure 5.- Concluded.
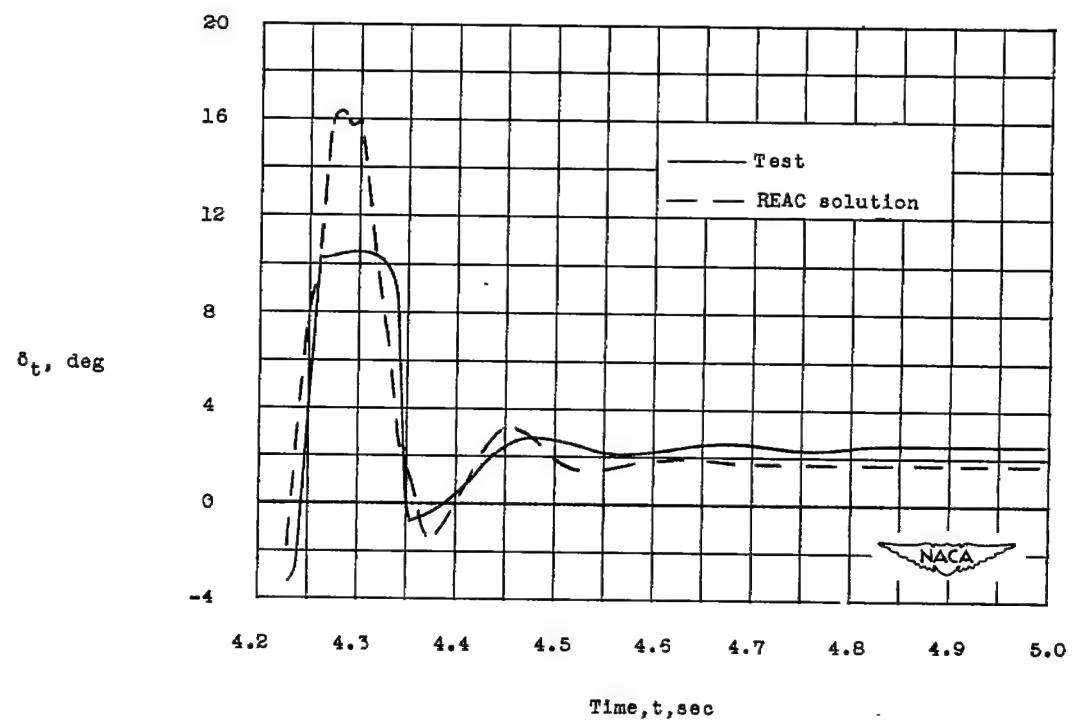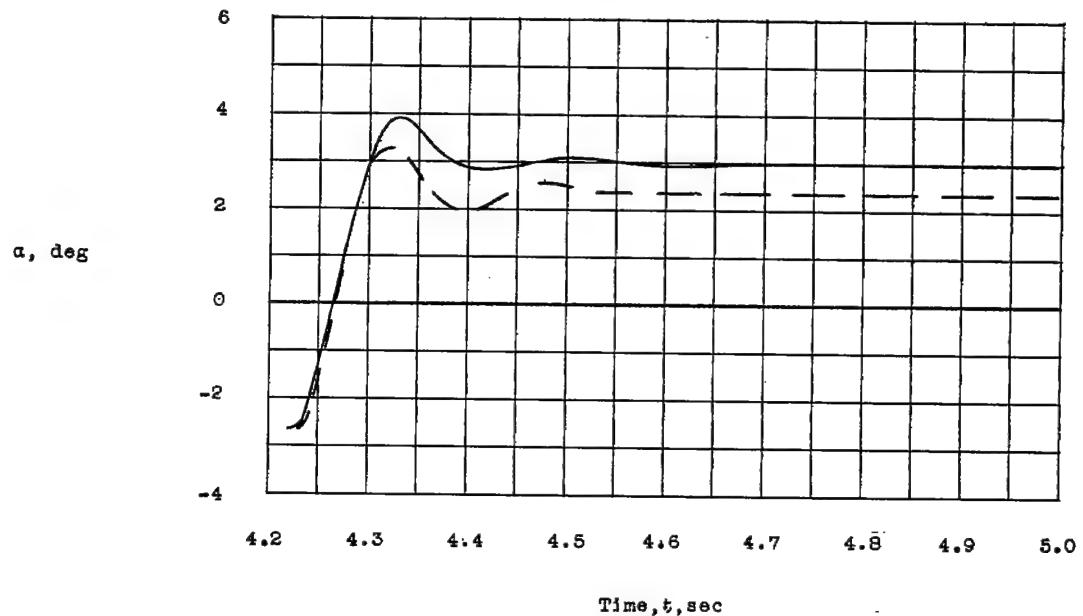
(a) M = 1.81.

Figure 6.- Measured and computed transient responses with rate damping.
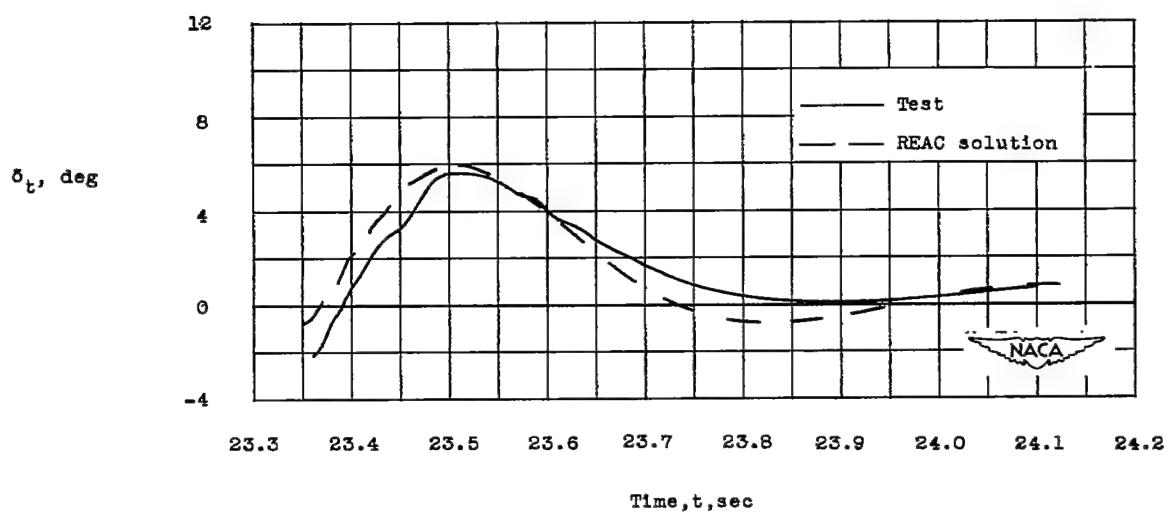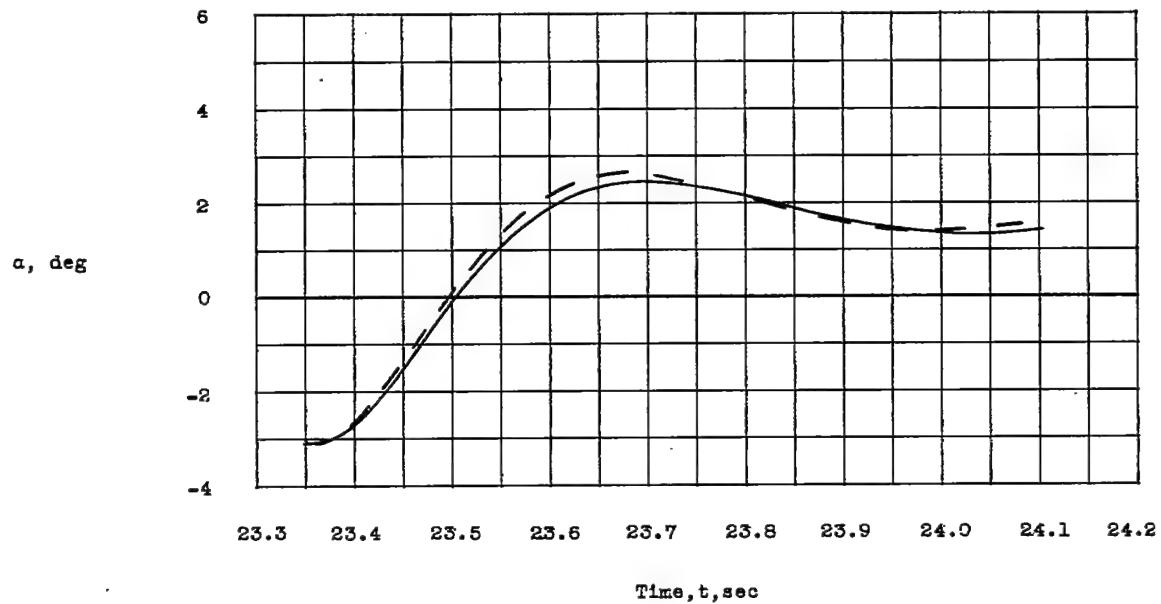
(b) M = 0.71.

Figure 6.- Concluded.
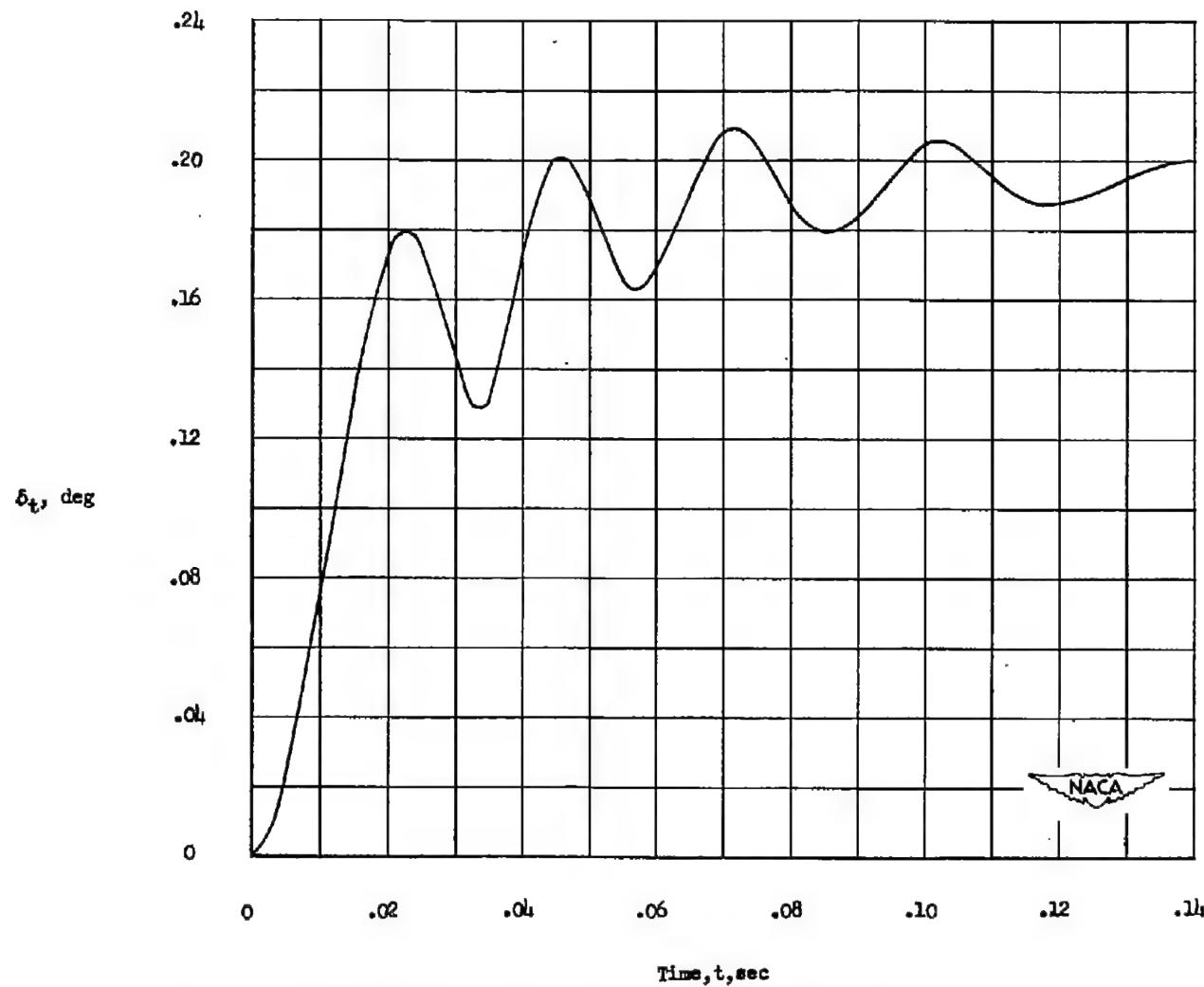
Figure 7.- Experimental rate-gyro-servo transient response to a unit pitching-velocity input.
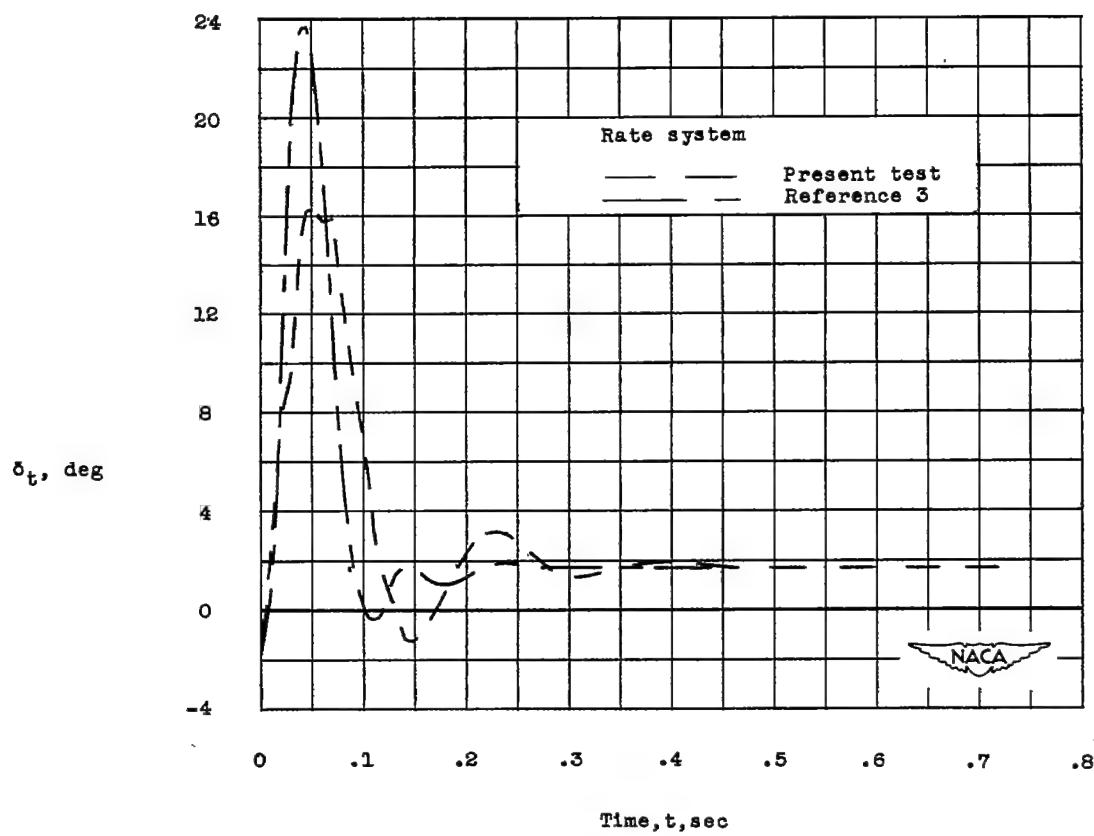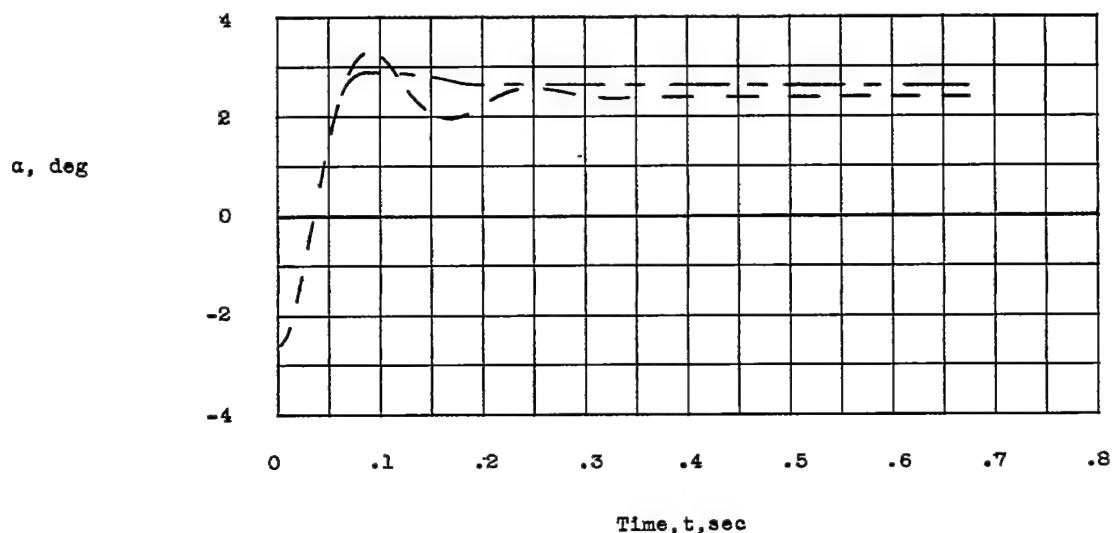
Figure 8.- Effect of rate-system dynamics on calculated model responses at a Mach number of 1.81.
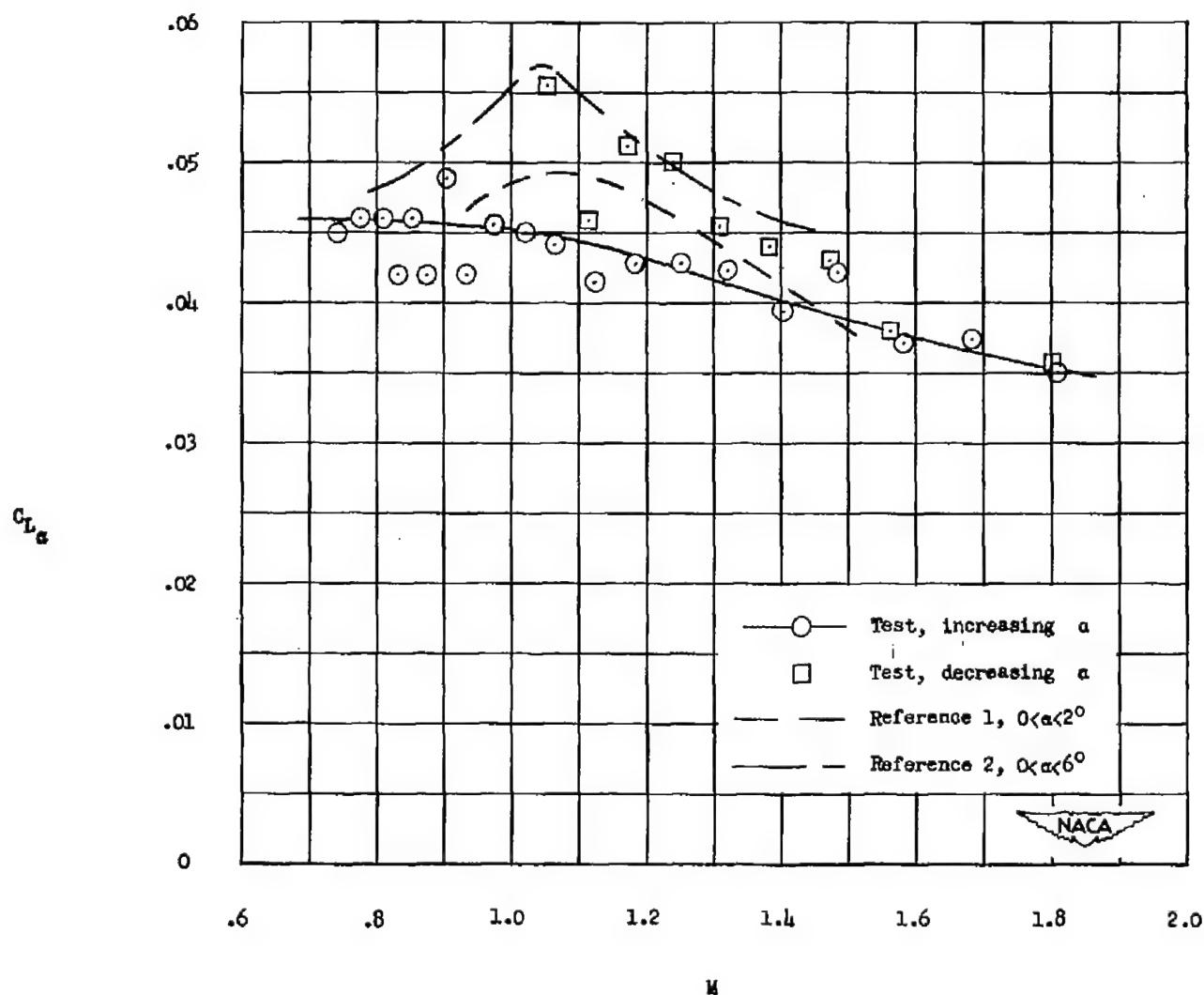
Figure 9.- Variation of lift-curve slope with Mach number.
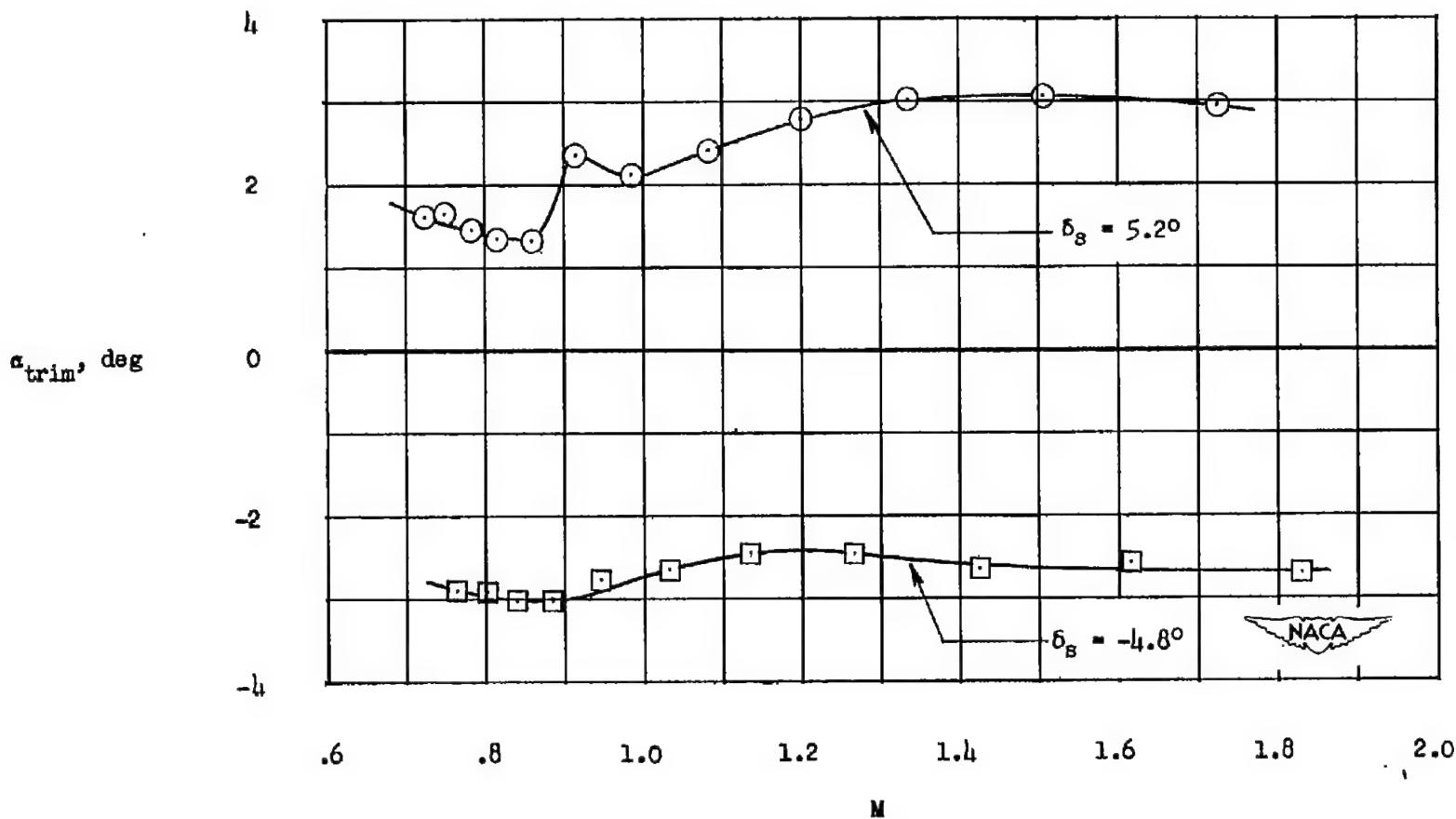
Figure 10.- Variation of trim angle of attack with Mach number.
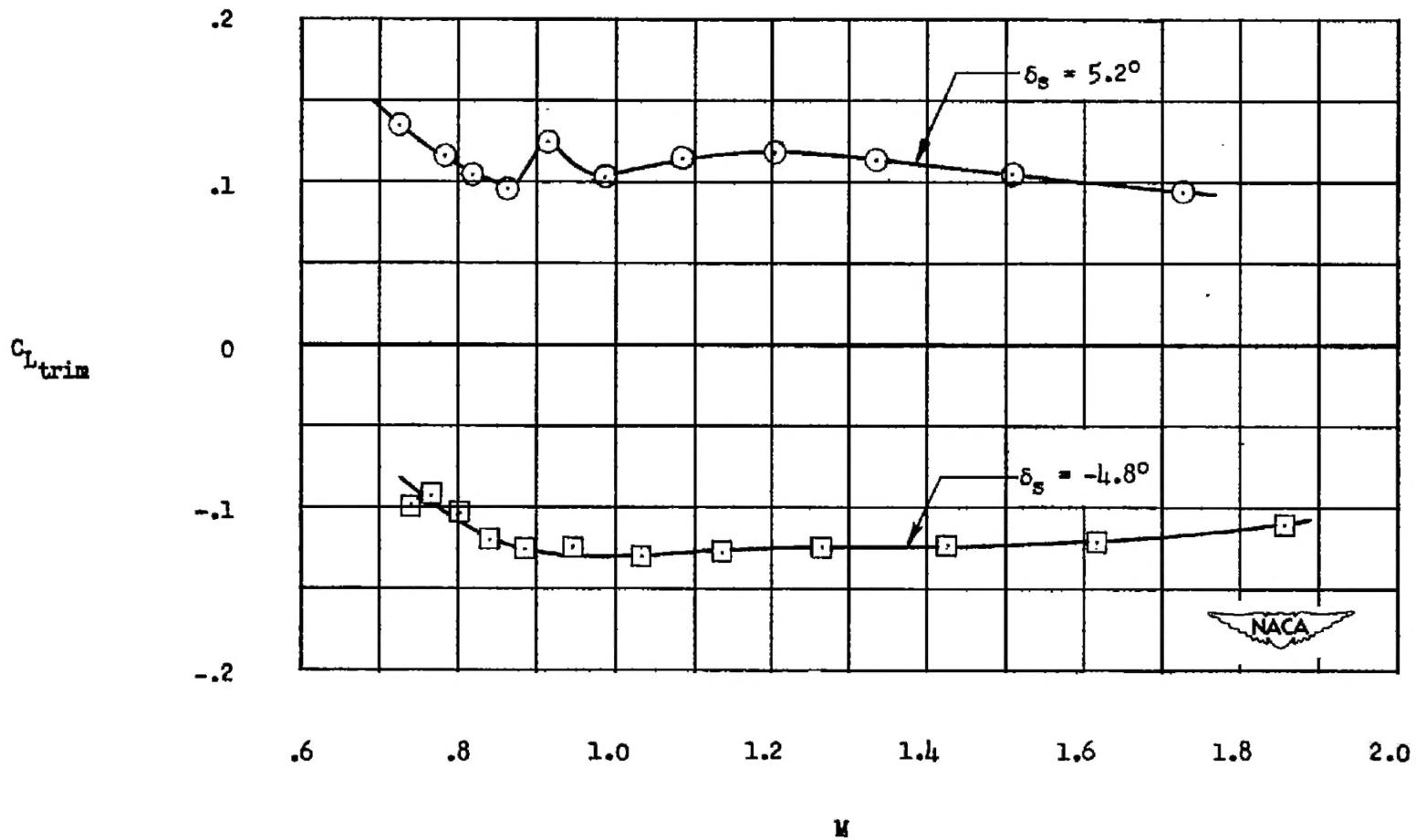
Figure 11.- Variation of trim lift coefficient with Mach number.
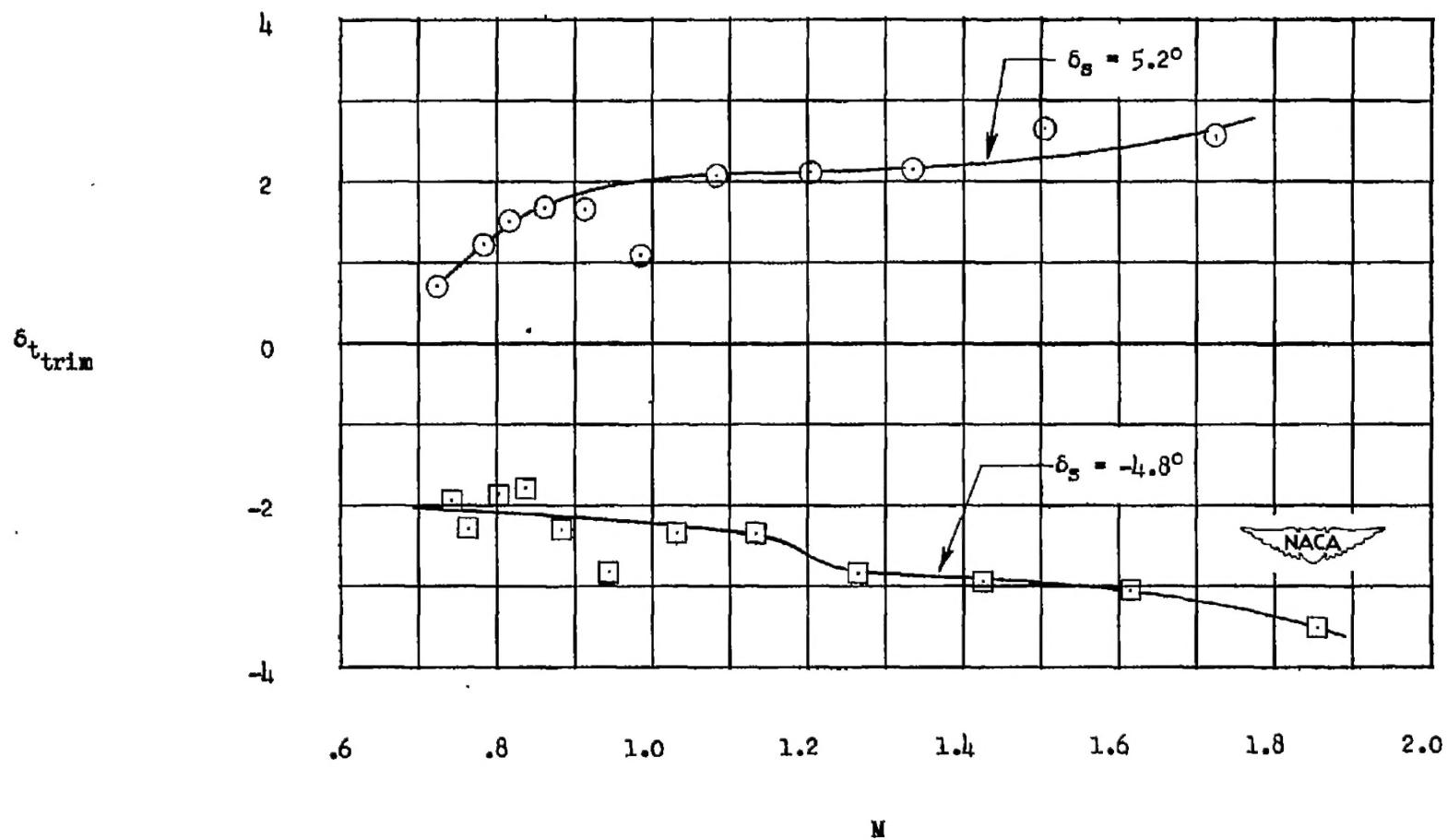
Figure 12.- Variation of trim tip-control deflection with Mach number.
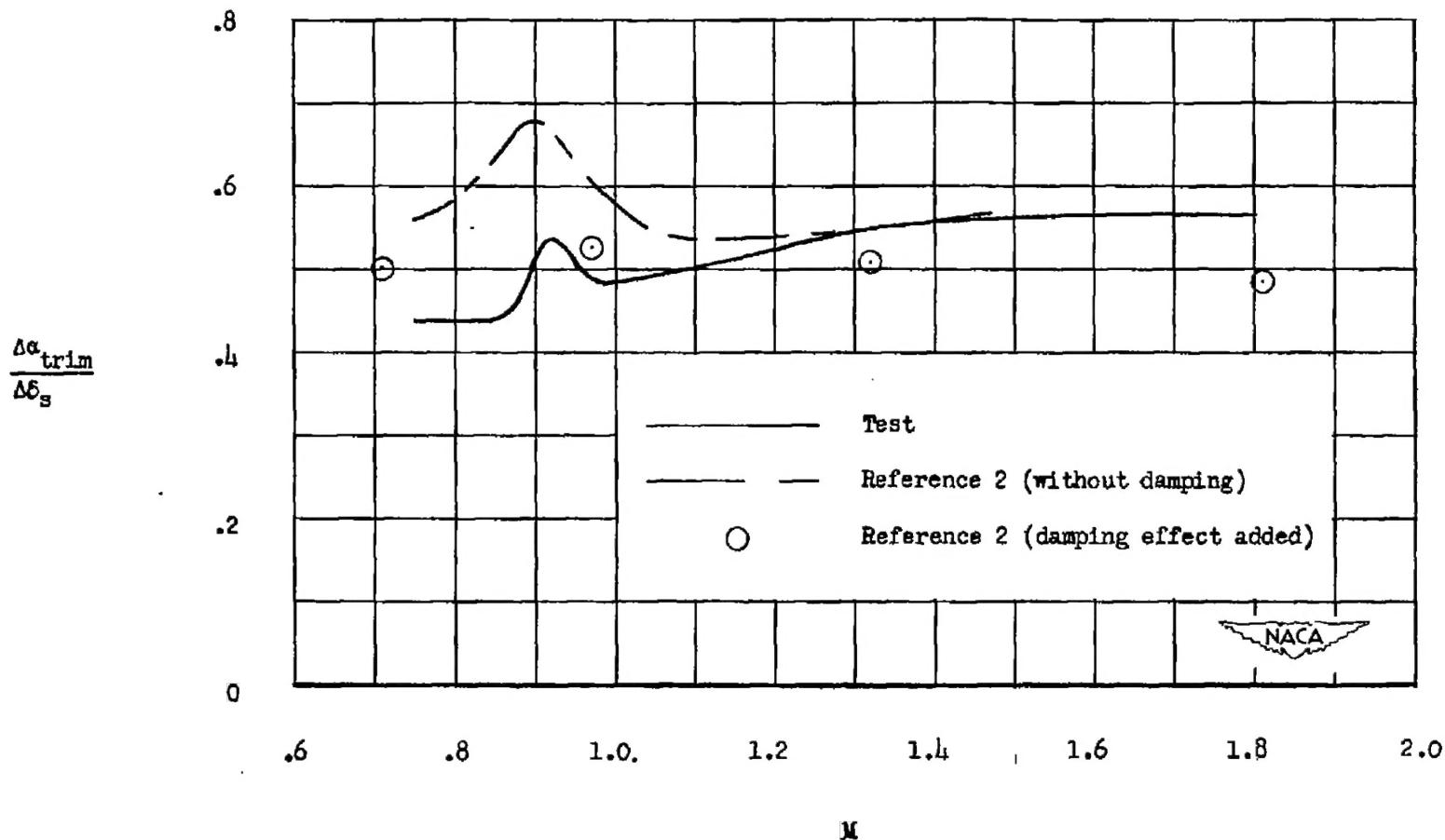
Figure 13.- Variation of trim angle of attack per unit control deflection
with Mach number.
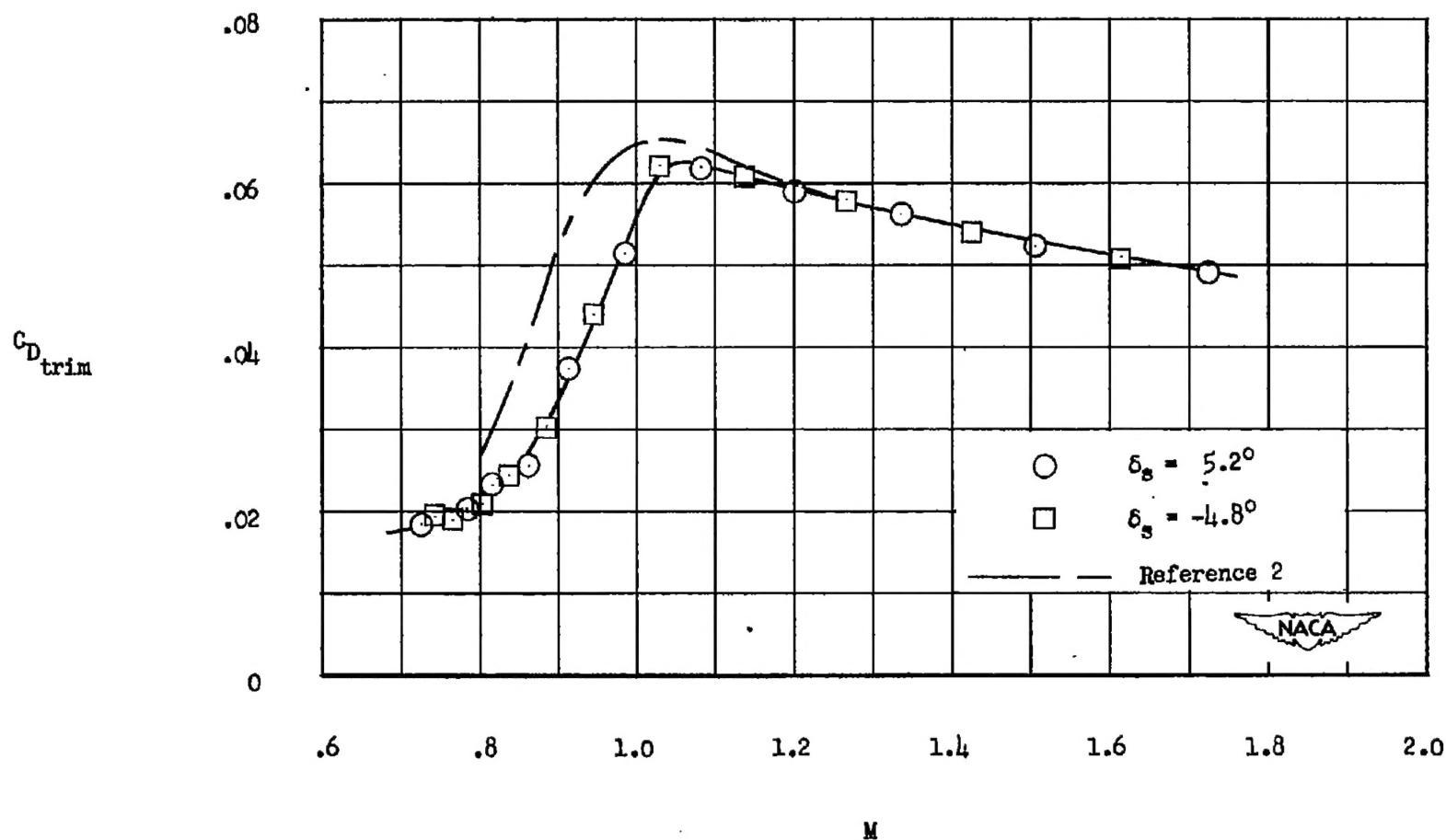
Figure 14.- Variation of trim drag coefficient with Mach number; $C_L \approx 0.1$.